Published in final edited form as:
Biochemistry. 2010 February 9; 49(5): 872–881. doi:10.1021/bi901751b.

The Ability of Rodent Islet Amyloid Polypeptide to Inhibit Amyloid Formation by Human Islet Amyloid Polypeptide Has Important Implications For the Mechanism of Amyloid Formation and the Design of Inhibitors.[+]

Ping Cao[§], **Fanling Meng**[§], **Andisheh Abedini**[‡], and **Daniel P Raleigh**[§,#,*]

[§] Department of Chemistry, State University of New York at Stony Brook, Stony Brook, New York 11794-3400

[‡] Division of Surgical Science, Department of Surgery, College of Physicians & Surgeons, Columbia University, New York, New York, USA

[#] Graduate Program in Biochemistry and Structural Biology, and Graduate Program in Biophysics, State University of New York at Stony Brook, Stony Brook, NY 11794

Abstract

Islet amyloid polypeptide (IAPP) is a 37-residue polypeptide hormone which is responsible for islet amyloid formation in type II diabetes. Human IAPP is extremely amyloidogenic while rat and mouse IAPP do not form amyloid *in vitro* or *in vivo*. Rat and mouse IAPP have identical primary sequences, but differ from the human polypeptide at six positions, five of which are localized between residues 20 to 29. The ability of rat IAPP to inhibit amyloid formation by human IAPP was tested and the rat peptide was found to be an effective inhibitor. Thioflavin-T fluorescence monitored kinetic experiments, transmission electron microscopy and circular dichroism showed that rat IAPP lengthened the lag phase for amyloid formation by human IAPP, slowed the growth rate, reduced the amount of amyloid fibrils produced in a dose dependent manner, and altered the morphology of the fibrils. The inhibition of human IAPP amyloid formation by rat IAPP can be rationalized by a model which postulates formation of an early helical intermediate during amyloid formation where the helical region is localized to the N-terminal region of IAPP. The model predicts that proline mutations in the putative helical region should lead to ineffective inhibitors as should mutations which alter the peptide peptide interaction interface. This was confirmed by testing the ability of A13P and F15D point mutants of rat IAPP to inhibit amyloid formation by human IAPP. Both these mutants were noticeably less effective inhibitors than wild type rat IAPP. The implications for inhibitor design are discussed.

[+]This work was supported by Grant NIH GM078114 to DPR.

[*] Author to whom correspondence should be addressed: Daniel P. Raleigh: telephone, 631-632-9547; fax: 631-632-7960; draleigh@notes.cc.sunysb.edu.

Supporting Information **Available:** The results of the sedimentation equilibrium studies of rat IAPP, plots of the derivative of the thioflavin-T fluorescence vs time, experimental CD spectra and calculated CD spectra of rat and human IAPP as well as 1:1, 2:1 and 5:1 mixtures of rat and human IAPP. The results of gel filtration experiments conducted on A13P-rat IAPP and F15D-rat IAPP. An AGADIR analysis of the helical propensity of rat IAPP, A13P rat IAPP, and F15D rat IAPP. This material is available free of charge via the Internet at http://pubs.acs.org.

Keywords

Islet Amyloid; IAPP; Amylin; Amyloid Inhibitor; Helical Intermediate; Mouse Models; Type II diabetes

Amyloid formation plays an important role in a broad range of human diseases, including Alzheimer's disease, Parkinson's disease, and type II diabetes (1-3). Islet amyloid polypeptide (IAPP), also known as amylin, is a 37-residue polypeptide co-locally produced with insulin and co-secreted by the pancreatic β-cells as a soluble monomer (4-9). IAPP is the major protein component of the pancreatic islet amyloid deposits often associated with type II diabetes (4-5). Formation of islet amyloid is believed to contribute to the pathology of the disease by promoting β-cell death, and there appears to be some correlation between the level of amyloid and the severity of the disease (10-15). Islet amyloid formation has also been proposed to be a potentially important complicating factor in islet cell transplantation (16-18).

The mature form of human IAPP has an amidated C-terminus and a disulfide bridge between residues Cys-2 and Cys-7 (Figure 1). Not all species form islet amyloid. In particular, human and nonhuman primates express a form of IAPP which can form amyloid fibrils but rodents do not (6,19). The primary sequences of rodent and human IAPP are very similar aside from the 20-29 region. Mouse and rat IAPP have the same sequence, and differ from the human protein at only six of 37 positions, five of which are located in the 20-29 region. There are three proline residues in this region of rat IAPP located at positions 25, 28, 29, while human IAPP has none. Other differences are replacement of His-18 in human IAPP with Arg-18 in the rat sequence and substitution of Phe at position 23 and Ile at position 26 of the human sequence with Leu-23 and Val-26 in rat IAPP. The sequence of the human and rat polypeptides are shown in Figure 1.

The details of amyloid formation are still not well understood despite considerable effort, but recent experimental studies have led to the interesting suggestion that amyloid formation by human IAPP may proceed via a helical intermediate (20-23). Monomeric IAPP is a fluxional molecule which does not adopt a compact structure in isolation, but a rapidly growing body of experimental evidence clearly shows that certain regions of the polypeptide have a tendency to transiently sample partial helical conformations. A propensity to preferential populated helical φ and ψ angles has been detected in NMR studies of both human and rat IAPP. The different studies reach slightly different conclusions about the exact boundaries of the partially helical region, but the broad consensus is that the region begins between residues 5 to 7 and extends to residues 20-22 or even further (24-26). Furthermore, it is well documented that helical structure can be promoted in the same region in IAPP by interactions with membranes, or with other proteins or by the addition of low levels of helix inducing cosolvents (22, 27-30).

A model for helix induced amyloid formation proposes that the initial oligomerization step is driven by the association of amphiphilic helices localized to a region starting between residues 5 to 7 and extending to around the vicinity of residues 20 to 24. (20-23). In this model, initial self association is driven by the thermodynamic linkage between peptide association and the formation of the helical structure; a process which is well documented in many protein association domains (31-32). The association leads to a high local concentration of the C-terminal region of the polypeptide and this segment is known to be extremely amyloidogenic (33). The model predicts that rat IAPP should be able to interact with the helical region of human IAPP but will inhibit amyloid formation since the C-terminal region of rat IAPP, (residues 22 to 37) contains multiple proline substitutions which will inhibit the conversion to β-structure. The model further predicts that mutations which destabilize the propensity to form

helical structure or disrupt the putative hydrophobic peptide peptide interaction interface should lead to less effective inhibitors.

Here we test if rat IAPP inhibits amyloid formation by human IAPP and examine two mutants designed to test the proposed model. A13P rat IAPP, in which a single proline is substituted into the putative helical region, and a second mutant, F15D rat IAPP, designed to alter the potential peptide peptide interaction interface were tested. Our studies confirm that rat IAPP is monomeric, and lacks stable well defined structure in aqueous solution. We show that rat IAPP is a moderate inhibitor of amyloid formation by human IAPP *in vitro* and its behavior compares favorably to other reported inhibitors. Rat IAPP lengthens both the lag phase and the growth phase of the fibril formation pathway and decreases the final amount of amyloid fibrils in a dose dependent manner. In contrast, the A13P rat IAPP and the F15D rat IAPP point mutants are noticeably less effective inhibitors.

Experimental Procedures

Peptide Synthesis

Human IAPP, rat IAPP, A13P rat IAPP and F15D rat IAPP were synthesized on a 0.25 mmol scale using an Applied Biosystems 433A peptide synthesizer, via 9-fluornylmethoxycarbonyl (Fmoc) chemistry. Solvents used were A.C.S. grade. Fmoc protected pseudoproline (oxazolidine) dipeptide derivatives were purchased from Novabiochem. All other reagents were purchased from Advanced Chemtech, PE Biosystems, Sigma, and Fisher Scientific. A 5-(4′-fmoc-aminomethyl-3′, 5-dimethoxyphenol) valeric acid (PAL-PEG) resin was used to form an amidated C-terminus. Standard Fmoc reaction cycles were used. The first residue attached to the resin, pseudoproline dipeptide derivatives, all β-branched residues, and all residues directly following a β-branched residue were double coupled (34). Peptides were cleaved from the resin using standard TFA methods.

Peptide Purification and Oxidation

Crude peptides were partially dissolved in 20% acetic acid (v/v), frozen in liquid nitrogen and lyophilized. This procedure was repeated several times prior to purification to increase solubility. Disulfide bond formation was induced via oxidation by DMSO (35). The peptide was dissolved in 100% DMSO and allowed to stand at room temperature for a minimum 5 hours. The dry peptides were then re-dissolved in 30% acetic acid (v/v) and purified via reversed-phase HPLC, using a Vydac C18 preparative column (10 mm × 250mm). A two-buffer system was used: buffer A consists of 100% H_2O and 0.045% HCl (v/v) and buffer B includes 80% acetonitrile, 20% H_2O and 0.045% HCl (v/v). HCl was utilized as the ion pairing agent instead of TFA since TFA can influence the rate of aggregation. Purity was checked by HPLC using a Vydac C18 reversed-phase analytic column (4.6mm × 250mm) before each experiment. This is important because IAPP can undergo spontaneous deamidation. Peptides were analyzed by mass spectrometry using a Bruker MALDI-TOF MS. Oxidized rat IAPP; expected 3921.3, observed 3921.6. Human IAPP; expected 3903.6, observed 3903.4. A13P rat IAPP; expected 3945.4, observed 3945.2. F15D rat IAPP; expected 3887.3, observed 3886.8.

Sample Preparation

A 1.6 mM peptide solution was prepared in 100% hexafluoroisopropanol (HFIP) and stored at -20°C. Amyloid formation was initiated by dilution of the stock solution as described below.

Thioflavin-T-Binding Kinetic Experiments

Thioflavin-T binding assays were used to measure the development of structurally ordered fibrils over time. All fluorescence experiments were performed on an Applied Phototechnology

fluorescence spectrophotometer using an excitation wavelength of 450 nm and an emission wavelength of 485 nm. The excitation and emission slits were 5 nm. A 1.0 cm cuvette was used and each point was averaged for 1 minute. Solutions were prepared by diluting filtered stock peptide solution into 20 mM Tris-HCl buffer and thioflavin-T solution immediately before the measurement. A GHP Acrodisc 13mm Syringe filter with a 0.45 μm GHP membrane was used. The conditions were 16 μM human IAPP, 25 μM Thioflavin-T in 2% HFIP, 25°C, pH 7.4 for all experiments. All solutions were stirred during these experiments in order to maintain homogeneity. For seeding experiments, a fibril solution was prepared by dilution of 17 μL of filtered stock solution into 20 mM Tris-HCl buffer to give a final concentration 16 μM. The solution was stirred for 80 minutes at 25°C, a time which is longer than that required to form amyloid fibrils. Aliquots of this solution were used to seed other solutions. The solution was used within 8 hours to ensure reproducibility of the seeding experiments. The concentration of the seeds was 1.6 μM in monomer units. The concentration of rat IAPP and rat IAPP mutants ranged from 16 μM to 160 μM depending upon the experiments.

Circular Dichroism (CD)

CD spectra were measured on an Applied Photophysics Chirascan circular dichroism spectrometer. For far-UV CD wavelength scans, the peptide solutions were prepared by diluting the filtered stock peptide into 20 mM Tris-HCl buffer at pH 7.4. The final peptide concentrations for far-UV CD experiments were 16 μM in 2% HFIP. Spectra were recorded from 190 to 260 nm at 1 nm intervals in a quartz cuvette of 0.1 cm path length at 25°C. CD experiments used the same stock solutions as the thioflavin-T fluorescence measurements.

Transmission Electron Microscopy (TEM)

TEM was performed at the Life Science Microscopy Center at the State University of New York at Stony Brook. TEM samples were prepared from the solutions used for the fluorescence measurements. 15 μL of the peptide solution was removed at the end of the kinetic runs and placed on carbon-coated formvar 200 mesh copper grid for 1 min and then negatively stained with saturated uranyl acetate for 1 min.

Analytical Ultracentrifugation (AUC)

Analytical ultracentrifugation was performed with a Beckman Optima XL-A analytical ultracentrifuge at 25°C using rotor speeds of 38,000 rpm (24h) and 48,000 rpm (24h). Apparent molecular masses were determined at initial peptide concentrations of 30, 60, 90 μM rat IAPP in 20 mM Tris-HCl buffer (pH 7.4). Six channels, 12 mm path length, charcoal-filled Epon cell with quartz windows were used. The absorbance was measured at 280 nm and ten scans were averaged. The partial specific volume (0.7278 mL g^{-1}) and solution density (1.003 g l^{-1}) were calculated from the software program SEDNTERP. The HeteroAnalysis program from the Analytical Ultracentrifugation Facility at the University of Connecticut was used for data analysis.

Gel Filtration

Gel filtration measurements were performed using an AKTA purifier 10 FPLC (GE Healthcare) at 4°C and a superdex 75 10/300 GL column. The flow rate was set to 0.5ml/min. Peptides were loaded at a concentration of 160 μM in 20 mM pH 7.4 Tris-HCl buffer. 20 mM Tris-HCl buffer (pH 7.4) with 0.15 M NaCl was used as buffer system. Wild type rat IAPP, which is monomeric under these conditions, was used as control at the same concentration.

Results and Discussion

Rat IAPP is monomeric in aqueous solution

Rat IAPP is well known not to form amyloid (19). The association state of rat IAPP was examined using analytical ultracentrifugation (AUC) because self-association even in the absence of amyloid formation could lead to apparent effects on the formation of human IAPP oligomers and fibrils. AUC experiments confirmed that rat IAPP is monomeric under the conditions of these studies (Supporting Information). The AUC data were fit well by an ideal single-species model with a molecular weight within 5% of the monomer molecular weight. The average apparent experimental molecular mass determined from multiple experiments with rat IAPP over the concentration range of 30 to 90 μM is 4102.0, and the expected mass is 3921.3. CD experiments confirmed that rat IAPP does not adopt well ordered structure under the conditions of our studies (Supporting Information).

Rat IAPP inhibits amyloid formation by human IAPP in a dose dependent manner

The ability of human IAPP and rat IAPP to form amyloid fibrils was first tested using thioflavin-T binding assays. Fluorescence detected thioflavin-T binding assays are the standard method used to monitor the time course of fibril formation (36). The dye experiences a significant increase in quantum yield upon binding to amyloid fibrils. The exact mode of binding is not known but the dye is believed to bind to grooves formed on the surface of amyloid fibrils by aligned rows of side chains. The data collected for human IAPP shows a typical IAPP fibrillization process with a lag phase of about 10 minutes followed by a growth phase and a final plateau in which fibrils are in equilibrium with soluble IAPP (Figure 2). TEM images recorded at the end point of the reaction display the classic features of human IAPP amyloid fibrils (Figure 3-A). However, the results of the rat IAPP experiment are strikingly different. As expected, based on past studies, no significant change in thioflavin-T fluorescence is observed over the entire time course of the reaction, and TEM images of the end product reveal that no fibrils was formed (Figure 3-B). CD spectra recorded at the end of the kinetic runs show that the human IAPP sample is rich in β-structure, while the rat peptide is not (Supporting Information).

Important early work used thioflavin-T assays to show that rat IAPP lengthened the lag phase of human IAPP and reduced the final fluorescence intensity, but a quantitative analysis of the progress curves has not been reported nor was the final morphology of the products examined (37). The ability of rat IAPP to inhibit amyloid formation by human IAPP was tested at various ratios of rat to human IAPP. A 1:1 mixture of rat and human IAPP exhibits a lag phase which is 2.5 times longer than observed for human IAPP alone and a small but reproducible decrease in the final thioflavin-T fluorescence intensity is detected (Figure 2). More dramatic effects are observed at higher ratios of rat IAPP to human IAPP. The lag phase is increased by approximately a factor of 3.3 for the 2:1 mixture of rat to human IAPP relative to the uninhibited human IAPP control. The lag phase increases monotonically with increasing rat IAPP concentration and is 10 fold longer for the 5:1 rat to human IAPP sample and 22 fold longer for the 10:1 rat to human IAPP sample relative to the value observed in the absence of rat IAPP. The final thioflavin fluorescence is also reduced in a dose dependent manner. The final fluorescence intensity is often used as a measure of the amount of amyloid formed, however, the intensity is also affected by a variety of factors and considerable caution should be applied before interpreting thioflavin-T fluorescence intensity as a direct read out of the amount of amyloid. The final fluorescence intensity of the human and rat IAPP 5:1 mixture decreased by 67% relative to sample of pure human IAPP and is reduced by 85% in the 10:1 rat to human IAPP sample. These results are not due to a change in the amount of human IAPP present since all samples contained the same amount of human IAPP. The rat peptide alone has no effect on the observable thioflavin-T fluorescence at all concentrations examined (16 to 160 μM).

Thioflavin-T assays can give false positives in inhibitor assays since a number of factors can lead to a loss of thioflavin-T fluorescence beside the direct inhibition of amyloid formation (38). Thus, it is critical to assay any potential inhibitors by an independent method. TEM images were recorded of aliquots from each reaction mixture which were collected at a time point when the final fluorescence has reached the steady-state value. Amyloid fibrils were present in the 1:1 rat human IAPP mixture, but fewer fibrils were detected in the other mixtures and the morphology was clearly different. In particular, the TEM images recorded for the rat human IAPP 5:1 and 10:1 mixtures showed significantly thinner fibrils (Figure 3 C-F).

Examination of the kinetic curves displayed in Figure 2 indicates that rat IAPP alters both the lag time and the growth phase. Figure 4A displays a plot of the length of the lag phase, which is defined here as the time required to achieve 10% of the final fluorescence intensity, and the T_{50} times. T_{50} is defined as the time needed to reach 50% of the final fluorescence intensity, and includes contributions from both the lag phase and the growth phase. A more quantitative measure of the effects upon the growth phase can be obtained by calculating the apparent maximum rate, which is the apparent rate at T_{50}. The calculation is easily performed by numerical differentiation of the kinetic progress curve. The kinetic curves were fit to an empirical function which described a sigmoidal curve and the resulting parameters were used to calculate a plot of the derivative dF(t)/dt, where F(t) represents the fluorescence intensity, vs time (Supporting Information). This plot gives T_{50} and the maximum rate, i.e. dF/dt at $t = T_{50}$. As the amount of rat IAPP increases, the rate at T_{50} decreases (Figure 4-B). These results quantitatively confirm that rat IAPP inhibits amyloid formation by lengthening both the lag phase and the growth phase.

Demonstration of an interaction between rat and human IAPP

Surface plasma resonance has been used to demonstrate an interaction between rat IAPP and surface immobilized biotinylated human IAPP (39). To test for a direct interaction between rat and human IAPP in solution, far-UV CD spectroscopy was employed. Spectra were taken when the final fluorescence intensity reached the plateau value at the same time point that the TEM images were recorded. The CD spectrum of human IAPP indicated significant amounts of β-sheet structure, while the spectrum of rat IAPP was consistent with a flexible largely unstructured polypeptide (Supporting Information). Spectra were also recorded for the various mixtures of human and rat IAPP and were compared to the spectrum expected for a non-interacting mixture of the two peptides. The expected spectrum is easily calculated as the appropriately weighted sum of the spectrum of the sample of pure human IAPP and the spectrum of the sample of pure rat IAPP. Any differences between the observed and calculated spectra provide direct evidence for an interaction between the two peptides. The experimental spectra of the mixtures clearly differ from spectra calculated for a non-interacting mixture of the two peptides (Supporting Information).

Human IAPP fibrils do not seed amyloid formation by rat IAPP

A characteristic feature of amyloid formation is that the reaction can be seeded by adding small amounts of preformed amyloid fibrils to a soluble sample of protein. The seeds act as templates for rapid fibril growth and lead to the by passing of the lag phase. Having demonstrated the interaction of rat IAPP with human IAPP, we next sought to determine if rat IAPP can bind to seeds made from human IAPP fibrils, thus we are asking the question, can human IAPP efficiently seed fibril formation by rat IAPP? Human IAPP fibrils formed at the end of a kinetic run with pure human IAPP were used to seed a solution of rat IAPP at a ratio of 10% seeds. Kinetic curves presented in Figure 5 demonstrate that mature human IAPP fibrils are not capable of seeding fibril formation by rat IAPP under these conditions. The fluorescence intensity of the mixture of rat IAPP with the human IAPP seeds is slightly higher than the rat IAPP reaction alone, but this is due to the fact that human amyloid fibril seeds bind to thioflavin-

T. The critical observation is that no significant change in thioflavin-T fluorescence is observed over the time course of the reaction. In contrast, addition of the human IAPP seeds to the human IAPP reaction abolished the lag phase as expected (Figure 5).

Point mutations which disrupt the putative helical region of rat IAPP or target its ability to interact with human IAPP lead to much less effective inhibitors

Our model for the mode of inhibition of human IAPP amyloid formation by rat IAPP proposes that the polypeptides interact via their respective N-terminal regions, and suggests that these interactions are mediated by helical association. The model predicts that mutations which reduce the propensity of rat IAPP to sample helical conformations should lead to a less effective inhibitor. Consequently, we prepared a point mutant of rat IAPP, A13P-rat IAPP, in which Ala-13, a residue near the center of the putative helical region is replaced by Pro. The substitution will significantly reduce the propensity of the polypeptide to sample helical conformations. As expected, the mutant is monomeric (Supporting Information) and CD indicates that it does not adopt a well structured conformation.

The mutant is less effective at inhibiting amyloid formation by human IAPP than is the rat polypeptide. Figure 6 displays the results of a set of thioflavin-T fluorescence monitored kinetic experiments conducted at various ratios of A13P rat IAPP to human IAPP. The time to reach 50% of the final fluorescence intensity, T_{50}, is 5.3 times longer for the 10:1 mixture of A13P rat IAPP and human IAPP relative to a sample of pure human IAPP. In contrast, a 10 fold excess of wild type rat IAPP increase the T_{50} value by almost 25 fold, thus by this criteria the mutant is 4.6 times less effective. The A13P rat IAPP mutant has no significant effect on the final thioflavin-T fluorescence intensity even when added at a 10 fold excess, while a 10 fold excess of the wild type rat polypeptide reduces the final thioflavin-T fluorescence by 85%. The mutant is also much less effective at inhibiting the growth rate. The maximum rat in the presence of a 10 fold excess of the A13P mutant is more than 55 times lager than the maximum rate observed in the presence of a ten fold excess of wild type rat IAPP. The mutant is also less effective than the wild type rat polypeptide when added at a 5:1 or 1:1 ratio. The kinetic data is summarized in table 1. TEM studies confirm the results of the kinetic experiments. TEM images of samples collected at the end of the respective kinetic runs are included in figure 6. Amyloid fibers are observed even for experiment conducted with a 10 fold excess of the mutant polypeptide, although they appear somewhat less numerous than observed in the presence of lower amounts of the A13P rat IAPP mutant. Both the 1:1 and 5:1 samples exhibit dense matts of fibrils.

The proline mutant will reduce the ability of the rat peptide to adopt helical structure (Supporting Information). A more subtle mutation might target the putative interaction interface while not completely disrupting helical structure. We choose to target Phe-15. This residue has been proposed to play an important role in the initial events of human IAPP self association and in insulin IAPP interactions (22, 40). The latter is particularly interesting in the context of inhibitor design since insulin is one of the most potent inhibitors of IAPP amyloid formation known (39-42). We replace Phe-15 by Asp. An Asp substitution was chosen because the mutation replaces a large residue with a small one and introduces a charge into what would be a hydrophobic interface. Thioflavin-T fluorescence assays demonstrate that the F15D rat IAPP is a much less effective inhibitor than wild type rat IAPP (Figure 7). When added in a 10 fold excess, the F15D rat IAPP mutant increases the T_{50} value relative to pure human IAPP by a little more than a factor of two compared to 25 fold effect observed with the wild type rat IAPP. The mutant has a modest effect on the final thioflavin-T fluorescence intensity with a 10 fold excess of mutant inhibitor leading to only a 15% decrease relative to the uninhibited value. The effect on the growth rate is also modest and a 10 fold excess of mutant inhibitor reduces the maximum rate by a factor of three relative to the value measured in the absence of

the inhibitor, while a 10 fold excess of the wild type rat polypeptide decrease the maximum rate by more than a factor of 55. The mutant is also less effective than the wild type inhibitor when added at a 5 fold excess or at 1:1 ratio (table 1). TEM images of the final reaction products are included in figure 7. Dense collections of amyloid fibers are observed for all samples including the one in which mutant inhibitor is present in 10 fold excess relative to human IAPP.

Both the A13P and F15D mutants have a significant effect on the ability of rat IAPP. It is formally possible that the effects could be indirect in the sense that the mutants might have the unanticipated effect of promoting self association of the inhibitor, thereby reducing the amount of inhibitor actually available to interact with human IAPP. This is an unlikely scenario but it is important to test for. Consequently, we examined the properties of the mutants at the highest concentration used, 160 μM. Gel filtration (Supporting Information) confirms that both peptides are monomeric while CD indicates that they do not adopt well ordered structure. Neither mutant binds thioflavin even at the highest concentration.

Conclusions

The data presented here demonstrates that rat IAPP inhibits amyloid formation by human IAPP, lengthening both the lag phase and the growth phase in a dose dependent manner and altering the morphology of the fibrils which are formed as well as reducing the final thioflavin-T fluorescence intensity. The rat peptide is a less effective inhibitor than some other variants of full length human IAPP which contain fewer substitutions (43-44). The potential mode of action of those peptides has not been discussed in the literature, but interestingly, they contain either a single proline mutation in the 20-29 region or double N-methyl substitutions in the same region. Thus they likely act in a very similar fashion to rat IAPP. The simplest possible rationalization of the reduced potency of rat IAPP relative to these variants is that the multiple substitutions in rat IAPP lead to a weaker interaction with human IAPP. Irrespective of the mechanistic details, the combination of a motif which can recognize pre-β-sheet species formed by human IAPP together with a segment which prevents β-sheet formation is likely to be a broadly applicable approach to the development of inhibitors of human IAPP amyloid formation. Although rat IAPP is less effective than some full length variants of human IAPP, it is as effective at inhibiting amyloid formation as a number of small molecules and peptide based inhibitors (45-48).

The behavior of the mutant rat peptides is consistent with our proposed model of rat IAPP's ability to inhibit amyloid formation. The model postulates that rat IAPP takes part in early oligomerization involving residues in the putative helical region. The proline substitution is located in the middle of that segment and proline is the most helix destabilizing of the coded amino acids. Thus the A13P substitution should lead to less effective protein protein interactions. Of course, the proline mutant might also exert some of its effects by directly disrupting protein protein interaction surfaces as well as by reducing helical propensity. The F15D mutant is far more conservative in terms of helical propensity, but is nonconservative in that it replaces large hydrophobic residue with a small charged residue. F15 has been proposed to be involved in the early oligomerization steps of amyloid formation (22,40) by participating in peptide peptide interactions. Our conceptual model proposes that rat IAPP inhibits amyloid formation by human IAPP because it substitutes for human IAPP in these initial steps. The model predicts that mutations which drastically alter the interaction interface should affect the ability of rat IAPP to act as an inhibitor. This is precisely what is observed with the F15D rat IAPP mutant. Interestingly, the F15D mutant appears to have a somewhat more pronounced affect on the ability of rat IAPP to act as an amyloid inhibitor. This may indicate that alteration of the hydrophobic nature of the putative peptide peptide interface is more important than reducing the helical propensity. Irrespective of the mechanistic details, the behavior of the two mutants is consistent with the proposed model.

The ability of rat IAPP has interesting implications for transgenic mouse models of islet amyloid as has been previously noted (37,49). A number of mouse and rat models have been developed which express human IAPP in order to investigate the adverse effects of human IAPP amyloid formation (14,37,50-58). However, if mouse IAPP inhibits amyloid formation by human IAPP *in vivo* as well as *in vitro*, then the results of transgenic mouse experiments which involve mouse models that are heterozygous for mouse and human IAPP may be misleading.

Supplementary Material

Refer to Web version on PubMed Central for supplementary material.

Acknowledgments

We thank Professor Martin Zanni, Dr. Chris Middleton and members of the Raleigh group for helpful discussions.

References

1. Chiti F, Dobson CM. Protein misfolding, functional amyloid, and human disease. Annu Rev Biochem 2006;75:333–366. [PubMed: 16756495]
2. Sipe JD. Amyloidosis. Crit Rev Cl Lab Sci 1994;31:325–354.
3. Selkoe DJ. Cell biology of protein misfolding: The examples of Alzheimer's and Parkinson's diseases. Nat Cell Biol 2004;6:1054–1061. [PubMed: 15516999]
4. Westermark P, Wernstedt C, Wilander E, Hayden DW, Obrien TD, Johnson KH. Amyloid fibrils in human insulinoma and islets of langerhans of the diabetic cat are derived from a neuropeptide-like protein also present in normal islet cells. Proc Natl Acad Sci USA 1987;84:3881–3885. [PubMed: 3035556]
5. Cooper GJS, Willis AC, Clark A, Turner RC, Sim RB, Reid KBM. Purification and characterization of a peptide from amyloid-rich pancreases of type-2 diabetic-patients. Proc Natl Acad Sci USA 1987;84:8628–8632. [PubMed: 3317417]
6. Cooper GJS. Amylin compared with calcitonin-gene-related peptide -structure, biology, and relevance to metabolic disease. Endocr Rev 1994;15:163–201. [PubMed: 8026387]
7. Kahn SE, Dalessio DA, Schwartz MW, Fujimoto WY, Ensinck JW, Taborsky GJ, Porte D. Evidence of cosecretion of islet amyloid polypeptide and insulin by beta-cells. Diabetes 1990;39:634–638. [PubMed: 2185112]
8. Marzban L, Trigo-Gonzales G, Zhu XR, Rhodes CJ, Halban PA, Steiner DF, Verchere CB. Role of beta-cell prohormone convertase (PC) 1/3 in processing of pro-islet antyloid polypeptide. Diabetes 2004;53:141–148. [PubMed: 14693708]
9. Sanke T, Bell GI, Sample C, Rubenstein AH, Steiner DF. An islet amyloid peptide is derived from an 89-amino acid precursor by proteolytic processing. J Biol Chem 1988;263:17243–17246. [PubMed: 3053705]
10. Lorenzo A, Razzaboni B, Weir GC, Yankner BA. Pancreatic-islet cell toxicity of amylin associated with type-2 diabetes-mellitus. Nature 1994;368:756–760. [PubMed: 8152488]
11. Clark A, Lewis CE, Willis AC, Cooper GJS, Morris JF, Reid KBM, Turner RC. Islet amyloid formed from diabetes-associated peptide may be pathogenic in type-2 diabetes. Lancet 1987;2:231–234. [PubMed: 2441214]
12. Hull RL, Westermark GT, Westermark P, Kahn SE. Islet amyloid: A critical entity in the pathogenesis of type 2 diabetes. J Clin Endocr Metab 2004;89:3629–3643. [PubMed: 15292279]
13. Clark A, Wells CA, Buley ID, Cruickshank JK, Vanhegan RI, Matthews DR, Cooper GJS, Holman RR, Turner RC. Islet amyloid, increased a-cells, reduced b-cells and exocrine fibrosis - quantitative changes in the pancreas in type-2 diabetes. Diabetes Res Clin Ex 1988;9:151–159.
14. Hayden MR, Karuparthi PR, Manrique CM, Lastra G, Habibi J, Sowers JR. Longitudinal ultrastructure study of islet amyloid in the HIP rat model of type 2 diabetes mellitus. Exp Biol Med 2007;232:772–779.

15. Kahn SE, Andrikopoulos S, Verchere CB. Islet amyloid: A long-recognized but underappreciated pathological feature of type 2 diabetes. Diabetes 1999;48:241–253. [PubMed: 10334297]
16. Westermark GT, Westermark P, Berne C, Korsgren O, Transpla NNCI. Widespread amyloid deposition in transplanted human pancreatic islets. New Engl J Med 2008;359:977–979. [PubMed: 18753660]
17. Westermark GT, Westermark P, Nordin A, Tornelius E, Andersson A. Formation of amyloid in human pancreatic islets transplanted to the liver and spleen of nude mice. Upsala J Med Sci 2003;108:193–203. [PubMed: 15000457]
18. Udayasankar J, Kodama K, Hull RL, Zraika S, Aston-Mourney K, Subramanian SL, Tong J, Faulenbach MV, Vidal J, Kahn SE. Amyloid formation results in recurrence of hyperglycaemia following transplantation of human IAPP transgenic mouse islets. Diabetologia 2009;52:145–153. [PubMed: 19002432]
19. Westermark P, Engstrom U, Johnson KH, Westermark GT, Betsholtz C. Islet amyloid polypeptide - pinpointing amino-acid-Residues linked to amyloid fibril formation. Proc Natl Acad Sci USA 1990;87:5036–5040. [PubMed: 2195544]
20. Abedini A, Raleigh DP. A role for helical intermediates in amyloid formation by natively unfolded polypeptides? Phys Biol 2009;6:15005.
21. Abedini A, Raleigh DP. A critical assessment of the role of helical intermediates in amyloid formation by natively unfolded proteins and polypeptides. Protein Eng Des Sel 2009;22:453–459. [PubMed: 19596696]
22. Wiltzius JJW, Sievers SA, Sawaya MR, Eisenberg D. Atomic structures of IAPP (amylin) fusions suggest a mechanism for fibrillation and the role of insulin in the process. Protein Sci 2009;18:1521–1530. [PubMed: 19475663]
23. Williamson JA, Loria JP, Miranker AD. Helix stabilization precedes aqueous and bilayer-catalyzed fiber formation in islet amyloid polypeptide. J Mol Biol 2009;393:383–396. [PubMed: 19647750]
24. Williamson JA, Miranker AD. Direct detection of transient alpha-helical states in islet amyloid polypeptide. Protein Sci 2007;16:110–117. [PubMed: 17123962]
25. Wei L, Jiang P, Yau YH, Summer H, Shochat SG, Mu YG, Pervushin K. Residual structure in islet amyloid polypeptide mediates its interactions with soluble insulin. Biochemistry 2009;48:2368–2376. [PubMed: 19146426]
26. Yonemoto IT, Kroon GJA, Dyson HJ, Balch WE, Kelly JW. Amylin proprotein processing generates progressively more amyloidogenic peptides that initially sample the helical state. Biochemistry 2008;47:9900–9910. [PubMed: 18710262]
27. Knight JD, Hebda JA, Miranker AD. Conserved and cooperative assembly of membrane-bound alpha-helical states of islet amyloid polypeptide. Biochemistry 2006;45:9496–9508. [PubMed: 16878984]
28. Jayasinghe SA, Langen R. Lipid membranes modulate the structure of islet amyloid polypeptide. Biochemistry 2005;44:12113–12119. [PubMed: 16142909]
29. Apostolidou M, Jayasinghe SA, Langen R. Structure of alpha-helical membrane-bound human islet amyloid polypeptide and its implications for membrane-mediated misfolding. J Biol Chem 2008;283:17205–17210. [PubMed: 18442979]
30. Nanga RPR, Brender JR, Xu JD, Veglia G, Ramamoorthy A. Structures of rat and human islet amyloid polypeptide IAPP(1-19) in micelles by NMR spectroscopy. Biochemistry 2008;47:12689–12697. [PubMed: 18989932]
31. Landschulz WH, Johnson PF, Mcknight SL. The leucine zipper - a hypothetical structure common to a new class of DNA-binding proteins. Science 1988;240:1759–1764. [PubMed: 3289117]
32. Oshea EK, Rutkowski R, Kim PS. Evidence That the Leucine Zipper Is a Coiled Coil. Science 1989;243:538–542. [PubMed: 2911757]
33. Nilsson MR, Raleigh DP. Analysis of amylin cleavage products provides new insights into the amyloidogenic region of human amylin. J Mol Biol 1999;294:1375–1385. [PubMed: 10600392]
34. Abedini A, Raleigh DP. Incorporation of pseudoproline derivatives allows the facile synthesis of human IAPP, a highly amyloidogenic and aggregation-prone polypeptide. Org Lett 2005;7:693–696. [PubMed: 15704927]

35. Abedini A, Singh G, Raleigh DP. Recovery and purification of highly aggregation-prone disulfide-containing peptides: Application to islet amyloid polypeptide. Anal Biochem 2006;351:181–186. [PubMed: 16406209]
36. Levine H. Thioflavine-T interaction with amyloid beta-sheet structures. Amyloid 1995;2:1–6.
37. Westermark GT, Gebre-Medhin S, Steiner DF, Westermark P. Islet amyloid development in a mouse strain lacking endogenous islet amyloid polypeptide (IAPP) but expressing human IAPP. Mol Med 2000;6:998–1007. [PubMed: 11474116]
38. Meng F, Marek P, Potter KJ, Verchere CB, Raleigh DP. Rifampicin does not prevent amyloid fibril formation by human islet amyloid polypeptide but does inhibit fibril thioflavin-T interactions: Implications for mechanistic studies beta-cell death. Biochemistry 2008;47:6016–6024. [PubMed: 18457428]
39. Jaikaran ETAS, Nilsson MR, Clark A. Pancreatic beta-cell granule peptides form heteromolecular complexes which inhibit islet amyloid polypeptide fibril formation. Biochem J 2004;377:709–716. [PubMed: 14565847]
40. Gilead S, Wolfenson H, Gazit E. Molecular mapping of the recognition interface between the islet amyloid polypeptide and insulin. Angew Chem Int Edit 2006;45:6476–6480.
41. Larson JL, Miranker AD. The mechanism of insulin action on islet amyloid polypeptide fiber formation. J Mol Biol 2004;335:221–231. [PubMed: 14659752]
42. Westermark P, Li ZC, Westermark GT, Leckstrom A, Steiner DF. Effects of beta cell granule components on human islet amyloid polypeptide fibril formation. Febs Lett 1996;379:203–206. [PubMed: 8603689]
43. Abedini A, Meng F, Raleigh DP. A single-point mutation converts the highly amyloidogenic human islet amyloid polypeptide into a potent fibrillization inhibitor. J Am Chem Soc 2007;129:11300. [PubMed: 17722920]
44. Yan LM, Tatarek-Nossol M, Velkova A, Kazantzis A, Kapurniotu A. Design of a mimic of nonamyloidogenic and bioactive human islet amyloid polypeptide (IAPP) as nanomolar affinity inhibitor of IAPP cytotoxic fibrillogenesis. Proc Natl Acad Sci USA 2006;103:2046–2051. [PubMed: 16467158]
45. Porat Y, Mazor Y, Efrat S, Gazit E. Inhibition of islet amyloid polypeptide fibril formation: A potential role for heteroaromatic interactions. Biochemistry 2004;43:14454–14462. [PubMed: 15533050]
46. Porat Y, Abramowitz A, Gazit E. Inhibition of amyloid fibril formation by polyphenols: Structural similarity and aromatic interactions as a common inhibition mechanism. Chem Biol Drug Des 2006;67:27–37. [PubMed: 16492146]
47. Scrocchi LA, Chen Y, Wang F, Han K, Ha K, Wu L, Fraser PE. Inhibitors of islet amyloid polypeptide fibrillogenesis, and the treatment of type-2 diabetes. Lett Pept Sci 2003;10:545–551.
48. Aitken JF, Loomes KM, Konarkowska B, Cooper GJS. Suppression by polycyclic compounds of the conversion of human amylin into insoluble amyloid. Biochem J 2003;374:779–784. [PubMed: 12812521]
49. Buxbaum JN. Animal models of human amyloidoses: Are transgenic mice worth the time and trouble? Febs Lett 2009;583:2663–2673. [PubMed: 19627988]
50. Butler AE, Jang J, Gurlo T, Carty MD, Soeller WC, Butler PC. Diabetes due to a progressive defect in beta-cell mass in rats transgenic for human islet amyloid polypeptide (HIP rat) - A new model for type 2 diabetes. Diabetes 2004;53:1509–1516. [PubMed: 15161755]
51. Yagui K, Yamaguchi T, Kanatsuka A, Shimada F, Huang CI, Tokuyama Y, Ohsawa H, Yamamura KI, Miyazaki JI, Mikata A, Yoshida S, Makino H. Formation of islet amyloid fibrils in beta-secretory granules of transgenic mice expressing human islet amyloid polypeptide amylin. Eur J Endocrinol 1995;132:487–496. [PubMed: 7711888]
52. Fox N, Schrementi J, Nishi M, Ohagi S, Chan SJ, Heisserman JA, Westermark GT, Leckstrom A, Westermark P, Steiner DF. Human islet amyloid polypeptide transgenic mice as a model of non-insulin-dependent diabetes-mellitus (niddm). Febs Lett 1993;323:40–44. [PubMed: 8495745]
53. Wong WPS, Scott DW, Chuang CL, Zhang SP, Liu H, Ferreira A, Saafi EL, Choong YS, Cooper GJS. Spontaneous diabetes in hemizygous human amylin transgenic mice that developed neither islet amyloid nor peripheral insulin resistance. Diabetes 2008;57:2737–2744. [PubMed: 18633116]

54. Hull RL, Shen ZP, Watts MR, Kodama K, Carr DB, Utzschneider KM, Zraika S, Wang F, Kahn SE. Long-term treatment with rosiglitazone and metformin reduces the extent of, but does not prevent, islet antyloid deposition in mice expressing the gene for human islet antyloid polypeptide. Diabetes 2005;54:2235–2244. [PubMed: 15983227]

55. Andrikopoulos S, Hull RL, Verchere B, Wang F, Wilbur SM, Wight TN, Marzban L, Kahn SE. Extended life span is associated with insulin resistance in a transgenic mouse model of insulinoma secreting human islet amyloid polypeptide. Am J Physiol-Endoc 2004;M 286:E862–E862.

56. Henson MS, Buman BL, Jordan K, Rahrmann EP, Hardy RM, Johnson KH, O'Brien TD. An in vitro model of early islet amyloid polypeptide (IAPP) fibrillogenesis using human IAPP-transgenic mouse islets. Amyloid 2006;13:250–259. [PubMed: 17107885]

57. Matveyenko AV, Butler PC. Islet amyloid polypeptide (IAPP) transgenic rodents as models for type 2 diabetes. Ilar J 2006;47:225–233. [PubMed: 16804197]

58. Andrikopoulos S, Verchere CB, Howell WM, Wight TN, Kahn SE. Evidence for islet amyloid fibril formation in a new mouse model of insulinoma producing and secreting human islet amyloid polypeptide. Diabetes 1998;47:A197–A197.

Abbreviations

AUC	Analytical Ultracentrifugation
CD	Circular Dichroism
IAPP	islet amyloid polypeptide
A13P-rIAPP	an Ala-13 to Pro mutant of rat IAPP
F15D-rIAPP	a Phe-15 to Asp mutant of rat IAPP
TEM	Transmission Electron Microscopy
TFA	trifluoroacetic acid
T_{50}	the time required to achieve 50% of the final thioflavin intensity in a kinetic experiment

(A) Human IAPP:

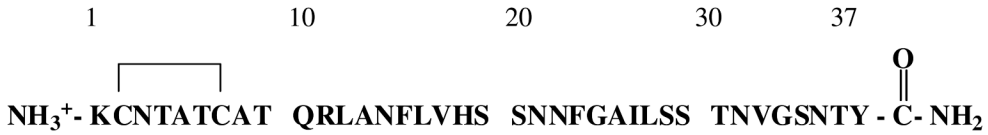

Rat IAPP:

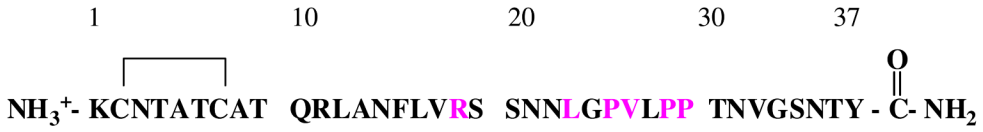

A13P Rat IAPP:

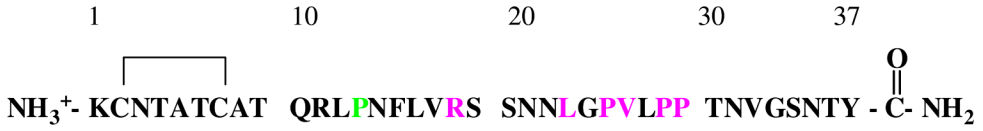

F15D Rat IAPP:

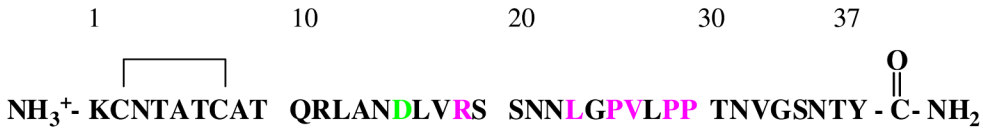

(B)

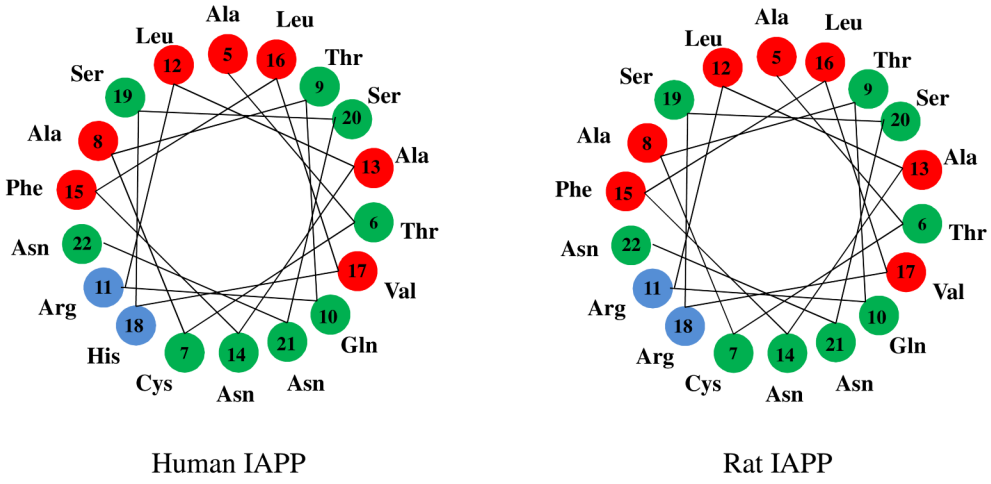

Figure 1.

Comparison of human and rat IAPP. (A) Primary sequence of human IAPP, rat IAPP and the A13P and F15D mutants of rat IAPP. All peptides have a disulfide bridge between Cys-2 and Cys-7 and have an amidated C-terminus. Residues which differ from the human peptide are colored in pink. Residues in the mutants which differ from wild type rat IAPP are colored in light green. (B) Helical wheel representation of residues 5 to 22 of human and rat IAPP. Red: nonpolar groups; green: polar, uncharged groups; blue: basic groups.

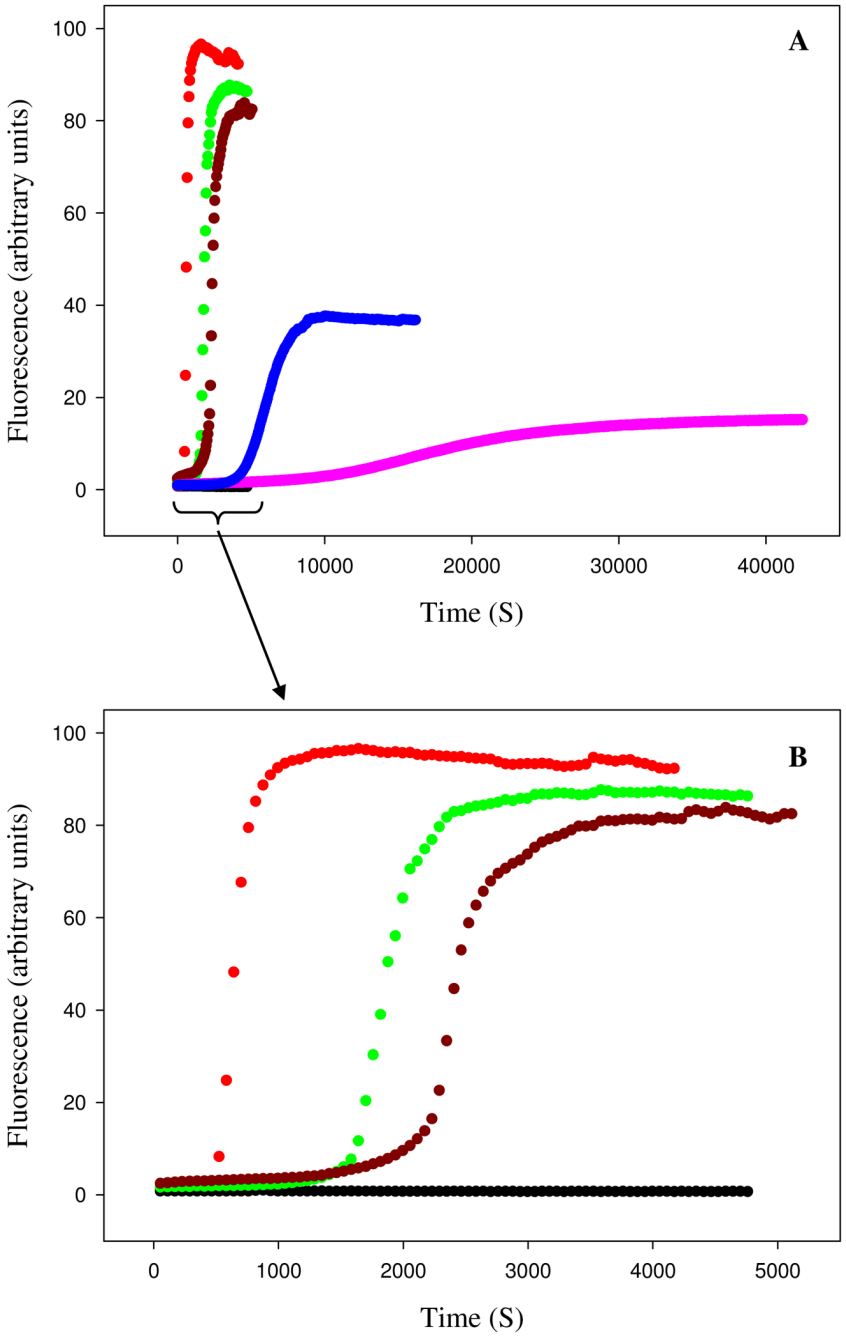

Figure 2.

Rat IAPP inhibits amyloid formation by human IAPP. (A) Fluorescence monitored thioflavin-T kinetic experiments are shown. Red, human IAPP; black, rat IAPP; green, rat IAPP : human IAPP at a 1:1 ratio; dark red, rat IAPP : human IAPP at a 2:1 ratio; blue, rat IAPP : human IAPP at a 5:1 ratio; pink, rat IAPP : human IAPP at a 10:1 ratio. (B) An expansion of the first 5000 sec of panel A for the pure human IAPP sample and the 1:1 and 2:1 mixtures of rat IAPP and human IAPP. All experiments were performed at 25°C, pH 7.4, 16 μM IAPP, 20 mM Tris-HCl, 25 μM thioflavin-T in 2% HFIP (v/v) with constant stirring. The concentration of rat IAPP ranged from 16 μM for the sample of pure rat IAPP and for the 1:1 ratio to 160 μM for the 10:1 ratio.

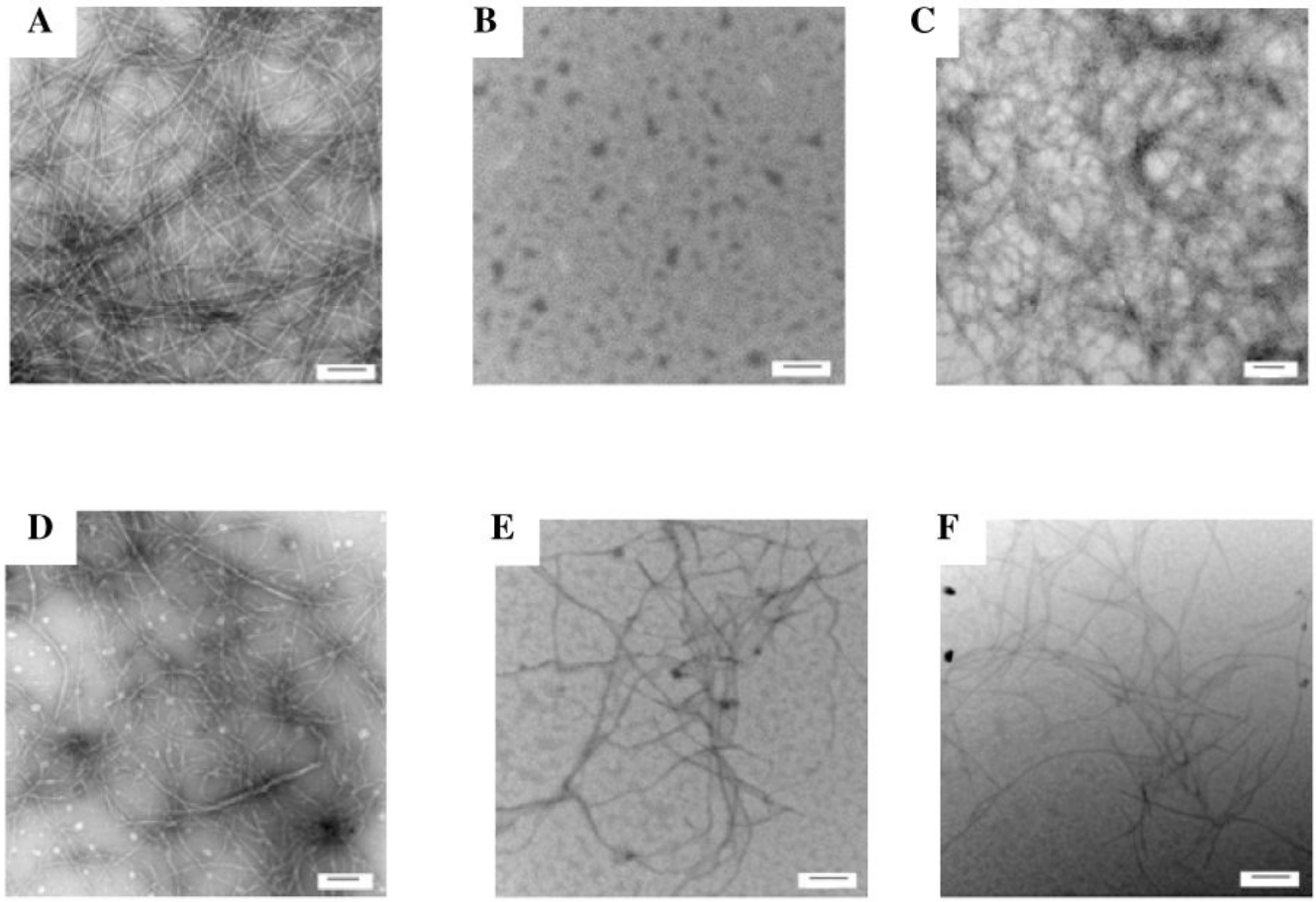

Figure 3.

Transmission electron microscopy confirms that rat IAPP inhibits amyloid formation by human IAPP. Samples were removed at the end of the kinetic reactions shown in figure-2 and TEM images recorded. (A) human IAPP; (B) rat IAPP; (C) 1:1 mixture of rat IAPP and human IAPP; (D) 2:1 mixture of rat IAPP and human IAPP; (E) 5:1 mixture of rat IAPP and human IAPP; (F) 10:1 mixture of rat IAPP and human IAPP. The scale bar represents 100 nm.

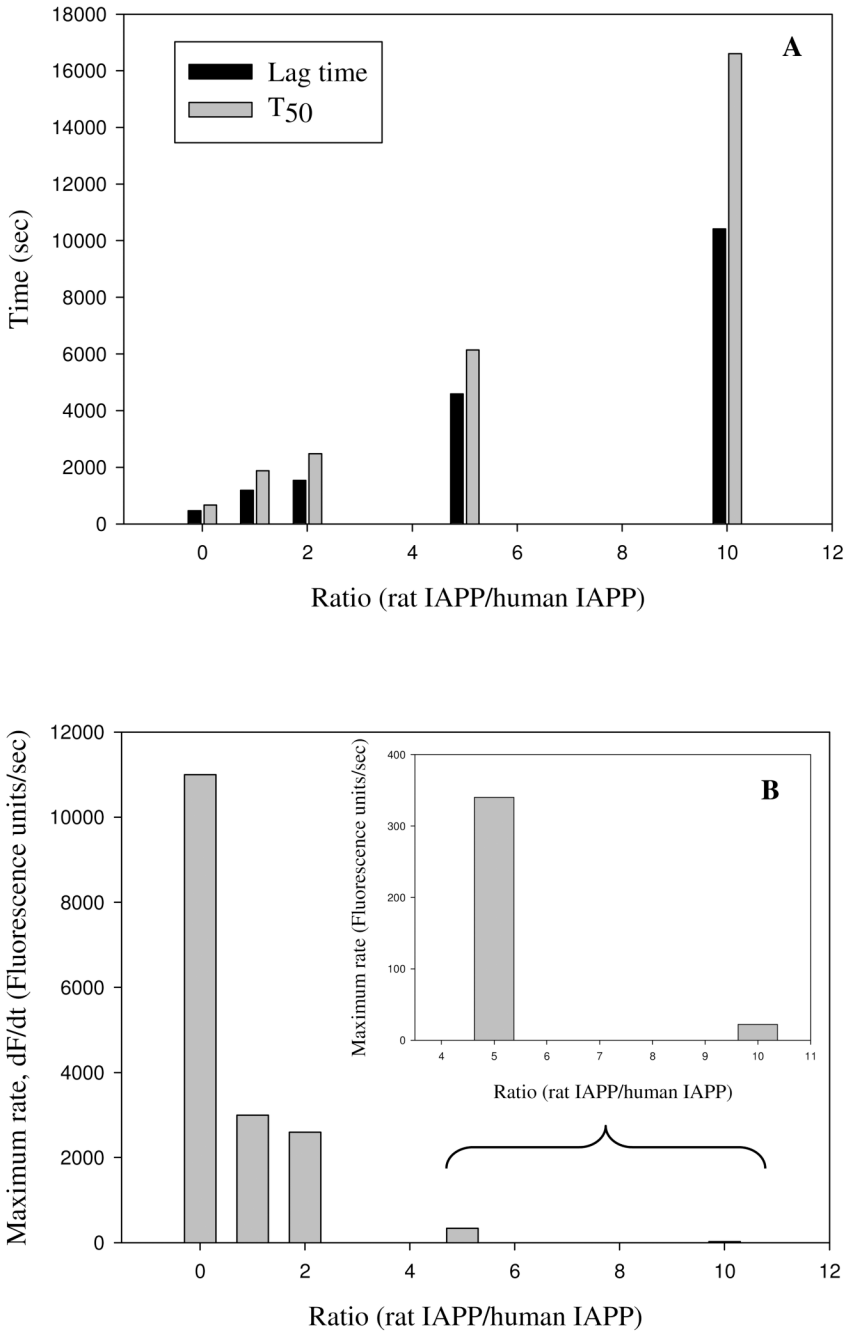

Figure 4.

The effect of rat IAPP on the lag phase and growth rate of human IAPP amyloid formation. (A) Rat IAPP lengthens the lag time for amyloid formation by human IAPP. The bar graph compares the experimental T_{50} time and lag time, for different ratios of rat to human IAPP ranging from 0 (pure human IAPP), to a 10 fold excess of rat IAPP (16 μM human IAPP and 160 μM rat IAPP). The lag time is defined as the time required to reach 10% of the final thioflavin-T fluorescence intensity. (B) Rat IAPP decreases the maximum rate of growth. The bar graph compares the maximum growth rate dF/dt, for different ratios of rat to human IAPP ranging from 0 (pure human IAPP), to a 10 fold excess of rat IAPP. The insert shows an expansion of the data for the 5:1 and 10:1 ratios.

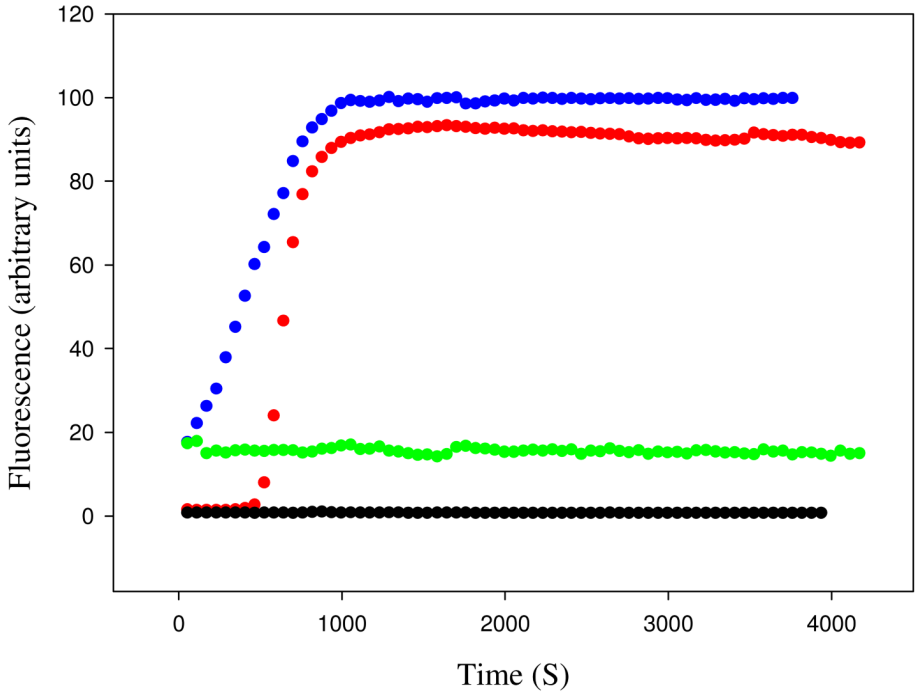

Figure 5.

Human IAPP amyloid fibrils do not seed amyloid formation by rat IAPP. Fluorescence monitored thioflavin-T kinetic experiments are shown. Red, unseeded human IAPP; black, unseeded rat IAPP; blue, human IAPP seeded by human IAPP fibrils; green, rat IAPP seeded by human IAPP fibrils. Experiments were performed at 25°C, pH 7.4, 20 mM Tris-HCl, 25 μM thioflavin-T in 2% HFIP (v/v) with constant stirring. The peptide concentration was 16 μM for human IAPP and 16 μM for rat IAPP. Human IAPP seeds, when added, were present at a monomer concentration of 1.6 μM.

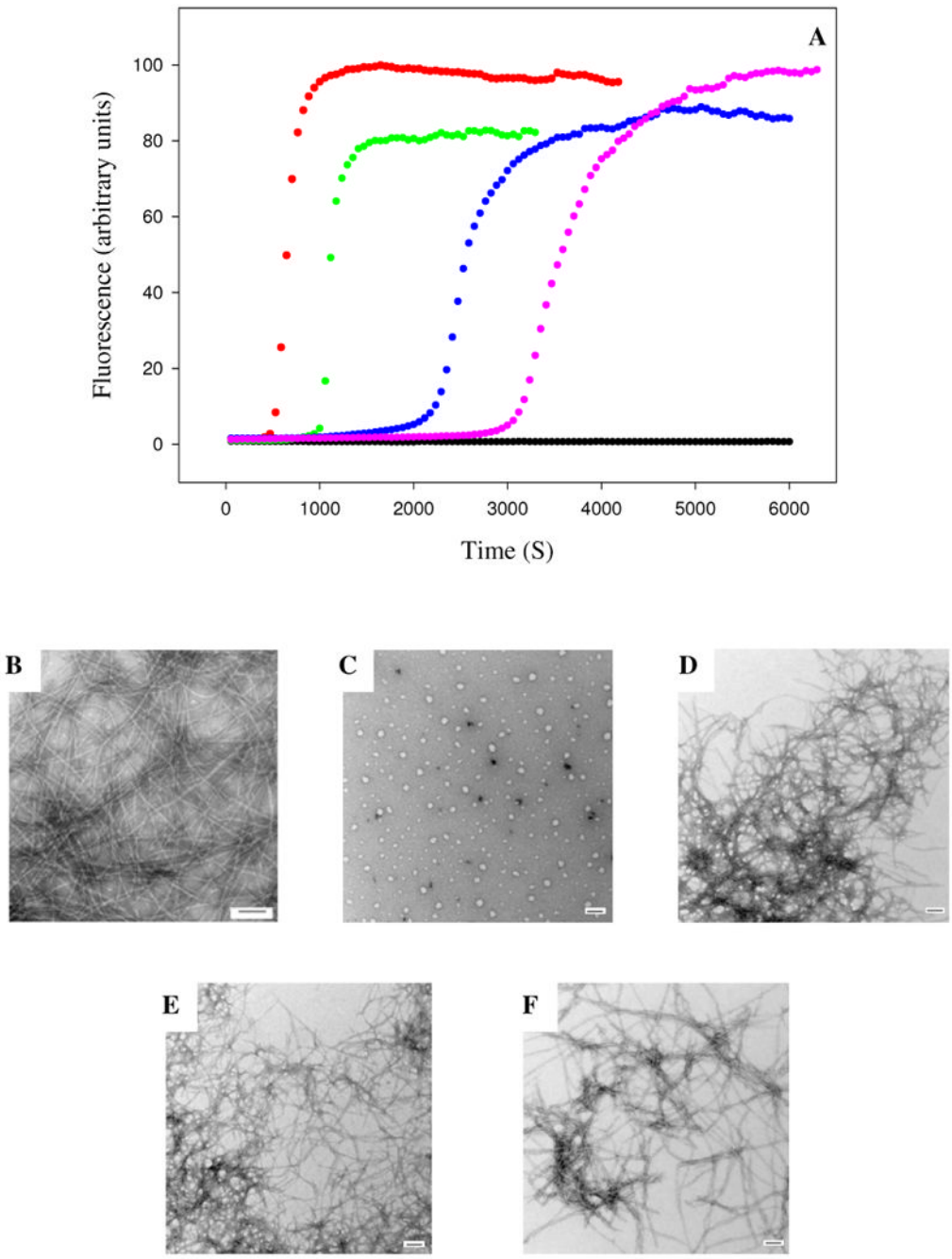

Figure 6.

The A13P mutant of rat IAPP is a less effective inhibitor of amyloid formation than wild type rat IAPP. (A) Fluorescence monitored thioflavin-T kinetic experiments are shown. Red, human IAPP; black, A13P rat IAPP; green, A13P rat IAPP : human IAPP at a 1:1 ratio; blue, A13P rat IAPP : human IAPP at a 5:1 ratio; pink, A13P rat IAPP : human IAPP at a 10:1 ratio. All experiments were performed at 25°C, pH 7.4, 16 μM IAPP, 20 mM Tris-HCl, 25 μM thioflavin-T in 2% HFIP (v/v) with constant stirring. The concentration of A13P rat IAPP ranged from 16 μM for the sample of pure A13P rat IAPP and for the 1:1 ratio to 160 μM for the 10:1 ratio. (B-F) Transmission electron microscopy confirms that A13P rat IAPP is a less effective inhibitor. Samples were removed at the end of the kinetic reactions and TEM images were

recorded. (B) human IAPP; (C) A13P rat IAPP; (D) 1:1 A13P rat IAPP : human IAPP; (E) 5:1 A13P rat IAPP : human IAPP; (F) 10:1 A13P rat IAPP : human IAPP.

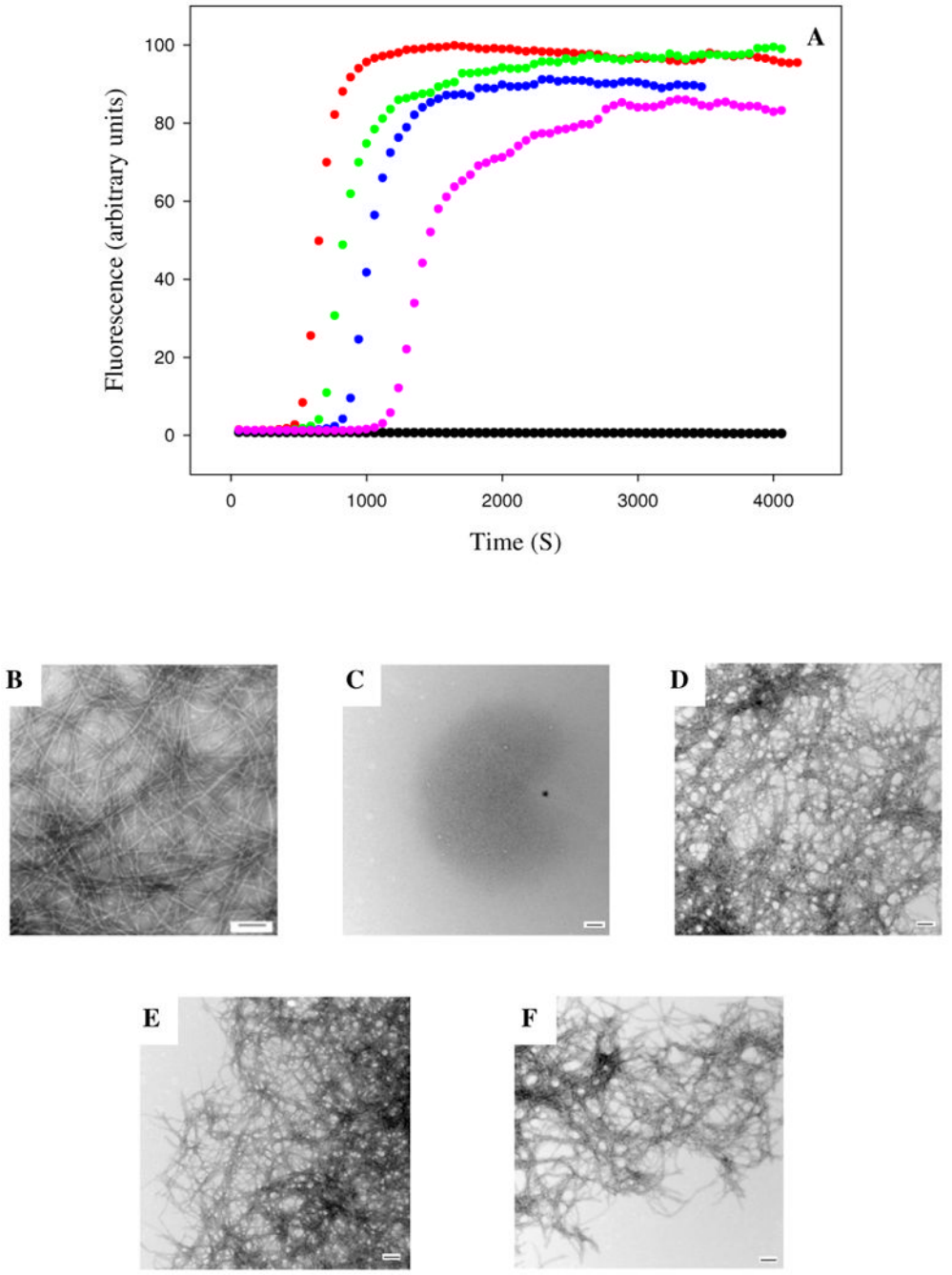

Figure 7.

The F15D mutant of rat IAPP is a less effective inhibitor of amyloid formation than wild type rat IAPP. (A) Fluorescence monitored thioflavin-T kinetic experiments are shown. Red, human IAPP; black, F15D rat IAPP; green, F15D rat IAPP : human IAPP at a 1:1 ratio; blue, F15D rat IAPP : human IAPP at a 5:1 ratio; pink, F15D rat IAPP : human IAPP at a 10:1 ratio. All experiments were performed at 25°C, pH 7.4, 16 μM IAPP, 20 mM Tris-HCl, 25 μM thioflavin-T in 2% HFIP (v/v) with constant stirring. The concentration of F15D rat IAPP ranged from 16 μM for the sample of pure F15D rat IAPP and for the 1:1 ratio to 160 μM for the 10:1 ratio. (B-F) Transmission electron microscopy confirms that F15D rat IAPP is a less effective inhibitor. Samples were removed at the end of the kinetic reactions and TEM images were

recorded. (B) human IAPP; (C) F15D rat IAPP; (D) 1:1 F15D rat IAPP : human IAPP; (E) 5:1 F15D rat IAPP : human IAPP; (F) 10:1 F15D rat IAPP : human IAPP.

Table 1

Comparison of kinetic parameters for human IAPP amyloid formation in the presence and in the absence of rat IAPP, and mutants of rat IAPP

Ratio of rat IAPP to human IAPP	Lag time (S)	T_{50} (S)	Maximum rate (Fluorescence units/sec)
pure human IAPP	470	670	11,000
1:1	1,180	1,870	3,000
2:1	1,530	2,480	2,600
5:1	4,590	6,140	340
10:1	10,410	16,600	22.0
Ratio of A13P rat IAPP to human IAPP	**Lag time (S)**	**T_{50} (S)**	**Maximum rate (Fluorescence units/sec)**
pure human IAPP	470	670	11,000
1:1	1,010	1,090	10,642
5:1	2,180	2,400	2,084
10:1	3,130	3,600	1,260
Ratio of F15D rat IAPP to human IAPP	**Lag time (S)**	**T_{50} (S)**	**Maximum rate (Fluorescence units/sec)**
pure human IAPP	470	670	11,000
1:1	700	830	6,773
5:1	880	1,010	6,319
10:1	1,200	1,400	3,402